[redacted]

Copy 1
RM SL54D09b

NACA

RESEARCH MEMORANDUM

for the

U. S. Air Force

FREE-FLIGHT ZERO-LIFT DRAG RESULTS FROM A 1/5-SCALE MODEL AND SEVERAL SMALL-SCALE EQUIVALENT BODIES OF REVOLUTION OF THE CONVAIR F-102 CONFIGURATION AT MACH NUMBERS UP TO 1.34

By Harvey A. Wallskog

Langley Aeronautical Laboratory
Langley Field, Va.

[redacted]

NATIONAL ADVISORY COMMITTEE
FOR AERONAUTICS

WASHINGTON
APR 14 1954

[redacted]

NATIONAL ADVISORY COMMITTEE FOR AERONAUTICS

RESEARCH MEMORANDUM

for the

U. S. Air Force

FREE-FLIGHT ZERO-LIFT DRAG RESULTS FROM A 1/5-SCALE MODEL AND SEVERAL SMALL-SCALE EQUIVALENT BODIES OF REVOLUTION OF THE CONVAIR F-102 CONFIGURATION AT MACH NUMBERS UP TO 1.34

By Harvey A. Wallskog

SUMMARY

A 1/5-scale, rocket-propelled model of the Convair F-102 configuration was tested in free flight to determine zero-lift drag at Mach numbers up to 1.34 and at Reynolds numbers comparable to those of the full-scale airplane. This large-scale model corresponded to the prototype airplane and had air flow through the duct. Additional zero-lift drag tests involved a series of small equivalent bodies of revolution which were launched by means of a helium gun. The several small-scale models tested corresponded to: the basic configuration, the 1/5-scale rocket-propelled model configuration, a 2-foot (full-scale) fuselage-extension configuration, and a 7-foot (full-scale) fuselage-extension configuration. Models designed to correspond to the area distribution at a Mach number of 1.0 were flown for each of these shapes and, in addition, models designed to correspond to the area distribution at a Mach number of 1.2 were flown for the 1/5-scale rocket-propelled model and the 7-foot-fuselage-extension configuration.

The value of external pressure drag coefficient (including base drag) obtained from the large-scale rocket model was 0.0190 at a Mach number of 1.05 and the corresponding values from the equivalent-body tests varied from 0.0183 for the rocket-propelled model shape to 0.0137 for the 7-foot-fuselage-extension configuration. From the results of tests of equivalent bodies designed to correspond to the area distribution at a Mach number of 1.0, it is evident that the small changes in shape incorporated in the basic and 2-foot-fuselage-extension configurations from that of the rocket-propelled model configuration will provide no significant change in pressure drag. On the other hand, the data from the 7-foot-fuselage-extension model indicate a substantial reduction in pressure drag at transonic speeds.

INTRODUCTION

The Convair F-102 airplane has been the subject of many tests made in the Naval Ordnance Laboratory 40 × 40 cm Aeroballistics Tunnel and the Southern California Cooperative Wind Tunnel by Convair and in the Langley 4- by 4-foot supersonic pressure tunnel and the Langley 8-foot transonic tunnel by the National Advisory Committee for Aeronautics. These tests, using small-scale models (1/20-scale and smaller), were performed to determine static stability, drag due to lift, and zero-lift drag of the basic airplane.

The present tests involve a 1/5-scale rocket-propelled model in which the primary objective was to obtain interference-free, zero-lift, external-drag data in free flight over the transonic speed range at Reynolds numbers near those encountered by the full-scale airplane. In addition to this large-scale test, several small equivalent bodies of revolution derived from the longitudinal distribution of cross-sectional area of the airplane at Mach numbers of 1.0 and 1.2 were flight tested by using a helium gun. These equivalent bodies were flown primarily as a quick and simple means of comparing drag-rise (that is, external pressure drag coefficient) values at transonic speeds of four proposed modifications to the F-102 configuration.

All models were designed (with the collaboration of the NACA) and built by Convair. All tests were conducted by the Langley Pilotless Aircraft Research Division and flight testing took place at the Langley Pilotless Aircraft Research Station at Wallops Island, Va. The present tests are a continuation of a research project conducted at the request of the U. S. Air Force.

SYMBOLS

X	longitudinal distance along body axis from station 0, in.
L	distance from station 0 to exit, in.
A	cross-sectional area of the particular configuration as determined by the intersecting Mach plane, sq in.
S	wing plan-form area obtained by extending the leading and trailing edges to the center line of the body, $S = 26.46$ sq ft for 1/5-scale model and $S = 0.1786$ sq ft for small-scale models

S_b base area of central body in the duct, 0.369 sq ft

A_i inlet area (interior, total for 2 inlets), 0.186 sq ft

A_e exit area, 0.186 sq ft

$\bar{c}$ mean aerodynamic chord, $\bar{c}$ = 4.63 ft for 1/5-scale model

α angle of attack, deg

β angle of sideslip, deg

M Mach number

q free-stream dynamic pressure, lb/sq ft

R Reynolds number (based on $\bar{c}$ for 1/5-scale model and L/12 for the small-scale models)

C_D total drag coefficient, $\frac{\text{Total drag force}}{qS}$

$C_{N_{trim}}$ trim normal-force coefficient, $\frac{\text{Trim normal force}}{qS}$

$C_{Y_{trim}}$ trim side-force coefficient, $\frac{\text{Trim side force}}{qS}$

H_e average total pressure across the duct near the exit, lb/sq ft

H_e/H_o pressure recovery, ratio of H_e to free-stream total pressure

p free-stream static pressure, lb/sq ft

p_b base pressure (on base of the duct central body only), lb/sq ft

C_{p_b} base pressure coefficient, $\frac{p_b - p}{q}$

C_{D_b} base drag coefficient, $-C_{p_b}\frac{S_b}{S}$

M_e Mach number at duct exit, $M_e = 1.0$ for $M > 1.0$ and M_e obtained from $\frac{p_e}{H_e} = \left(1 + 0.2M_e^2\right)^{-7/2}$ for $M < 1.0$

p_e static pressure at duct exit, $p_e = 0.5283H_e$ for $M > 1.0$ and $p_e = p_b$ for $M < 1.0$, lb/sq ft

m/m_o mass-flow ratio, $\frac{p_e M_e A_e}{pMA_i}\left(\frac{1 + 0.2M_e^2}{1 + 0.2M^2}\right)^{1/2}$

C_{D_I} internal-drag coefficient,

$$2\frac{m}{m_o}\frac{A_i}{S}\left[1 - \frac{M_e}{M}\left(\frac{1 + 0.2M^2}{1 + 0.2M_e^2}\right)^{1/2}\right] - \frac{(p_e - p)}{q}\frac{A_e}{S}$$

C_{D_f} friction-drag coefficient

C_{D_E} forebody external-drag coefficient, $C_D - C_{D_I} - C_{D_b}$

C_{D_p} forebody external-pressure-drag coefficient, $C_D - C_{D_I} - C_{D_b} - C_{D_f}$

$C_{D_{p+b}}$ external-pressure-drag coefficient, $C_D - C_{D_I} - C_{D_f}$, for 1/5-scale model, and $C_D - C_{D_f}$, for small-scale models

MODELS AND TESTS

Large-Scale Model

Figure 1 presents the general arrangement and geometry of the 1/5-scale rocket-propelled model of the Convair F-102 configuration. Also included in figure 1 is a plot which shows the longitudinal distribution of cross-sectional area of the complete model derived for Mach number 1.0 (planes normal to the reference line). Photographs of the model appear in figure 2. Pertinent dimensional data are listed in table I, and weight, balance, and inertia values are presented in table II.

The outside contour of the fuselage of the rocket-propelled model was formed by a heavy fiber glass and plastic skin which was secured to aluminum bulkheads. The internal duct was in the form of a Y where the branches merged a short distance behind the inlets to form a large single duct which surrounded the internal rocket motor. In the region of the duct exit, a conical-shaped sleeve was mounted around the rocket-motor nozzle to form a choking cup, thus providing an annular exit area (see figs. 1(b) and 2(c)). The choking cup was designed to provide an exit-to-inlet-area ratio of 1.0, where the reference inlet area was taken as the cross-sectional area in a plane normal to the duct axis at the most forward station where the interior contour is fully developed. The wing panels and vertical tail were formed by laminated wood with duralumin plates inlaid on the outer surfaces for strength and stiffness. The canopy, inlets, control-actuator housings, drogue parachute housing, wing fences, and wing-tip recognition lights were all scaled from the airplane. The entire model was finished with a heat-resistant, phenolic resin base paint.

A two-stage propulsion system, utilizing solid-fuel rocket motors, was used to launch the model from the ground and accelerate it to supersonic speeds. A general view of the model and booster-rocket combination taken just before launching appears in figure 2(d). The booster rocket propelled the model to a low subsonic speed at which time it separated from the model and the internal rocket was ignited and accelerated the model up to maximum speed ($M \approx 1.35$). The data contained herein were recorded during the period after the internal rocket-motor propellant was expended when the model was in free flight.

Small-Scale Models

Details of the equivalent bodies of revolution representing the several modified airplane shapes which were under consideration are presented in figure 3. Models 1 to 6 correspond to the following full-scale airplane configurations:

	Model
Basic configuration	1
1/5-scale rocket-propelled model configuration (present large-scale test)	2 and 5
2-foot (full-scale) fuselage extension	3
7-foot (full-scale) fuselage extension	4 and 6

Models 1 to 4 were transonic ($M = 1.0$) area-rule models, that is, the cross-sectional areas (fig. 3(b)) were determined by planes intersecting the airplane perpendicular to the reference axis. Models 5 and 6 corresponded to the area distributions of the respective airplanes as determined by planes which intersected the reference axis at an angle equal

to the slope of the Mach line at a Mach number of 1.2. The final area distributions of the models corresponding to M = 1.2 (figs. 3(c) and (d)) were obtained from the average, at each longitudinal station, of the areas defined by each of the oblique cuts projected on a plane perpendicular to the reference axis taken at 10 angles of roll between 0° and 180°. The model bodies were made so that the total of the cross-sectional area of the body and stabilizing fins was equal to the total area less duct inlet area of the corresponding airplane at the same station.

The models were machined in two parts, a steel nose and an aluminum afterbody. The hexagonal-section, swept stabilizing fins were made of duralumin and pinned in place. Photographs of typical models appear in figure 4.

The models were launched to supersonic speeds using the helium gun which is described in reference 1.

INSTRUMENTATION AND DATA REDUCTION

Large-Scale Model

The 1/5-scale rocket-propelled model was equipped with an 8-channel telemeter contained within the body which transmitted continuous measurements of longitudinal, normal, and transverse accelerations, free-stream, duct-inlet, and duct-exit total pressures, and static pressures in the duct at the exit and on the base of the choking cup. The three accelerometers were located near the model center of gravity and the total-pressure probe in the duct near the exit was a slotted, integrating rake spanning the duct (see fig. 1(b)). The measurements of duct-inlet total pressure and duct-exit static pressure were of questionable quality and hence were not used to obtain the internal-drag and duct-pressure-recovery data presented herein. Other instrumentation used to record necessary information consisted of an NACA modified SCR-584 radar tracking unit for measuring trajectory and a radiosonde unit used to measure air pressure and temperature from which local values of the speed of sound, density, viscosity, and altitude were obtained.

Model airspeeds, Mach numbers, and dynamic pressures were calculated from telemetered values of free-stream total pressures and ambient pressures from the radiosonde survey. Reynolds numbers were obtained from a combination of telemeter and radiosonde data. Longitudinal-, normal-, and side-force coefficients (C_D, C_N, and C_Y, respectively) were obtained using telemetered values of acceleration. In the case of C_D, deviations from the standard method of data reduction are explained in the following paragraph.

Pressure-recovery data at the duct exit (H_e/H_o) are presented because of the lack of inlet total-pressure data. Mass-flow ratios (m/m_o) and internal-drag coefficients were obtained by assuming that for free-stream Mach numbers greater than 1.0 the duct-exit Mach number was equal to 1.0. Further, it was assumed that for subsonic flight the base-pressure measurement could be substituted for the duct-exit static pressure.

In the case of the present 1/5-scale model the telemetered signal corresponding to the longitudinal-acceleration instrument apparently suffered an abrupt shift and a drift in frequency which was proportional to acceleration. The magnitude of the shift and drift in acceleration was calculated by using unpublished subsonic external-drag-coefficient data from tests of the F-102 configuration conducted in the Langley 8-foot transonic tunnel. By using these data (after adjustment for Reynolds number difference by means of ref. 2) at two subsonic Mach numbers and by applying the actual test conditions of the rocket model, it was possible to correct the telemetered values of longitudinal acceleration. By comparing the calculated and telemetered values of longitudinal acceleration at the two subsonic Mach numbers and assuming the drift rate to be constant, it was possible to calculate the shift and drift rate which occurred in flight. The reduction of total-drag data was stopped at $M = 0.75$ because at lower Mach numbers the drift was nonlinear.

The total-drag-coefficient data contained herein are believed to be accurate to within ± 0.0015 in C_D and ± 0.010 in M. In addition, it is believed that adjustment of the data in the manner described previously had little detrimental effect on the measurement of the drag rise. Unpublished data from another large-scale, free-flight test of a modified configuration of the F-102 airplane substantiate the subsonic-drag-coefficient level of the present tests.

Small-Scale Models

Data were obtained for the small-scale equivalent-body models by the use of a CW Doppler radar unit which was located on the ground next to the gun. Total drag coefficients and Mach numbers were determined by means of these radar data and measured ground pressure and temperature by the method described in reference 3.

The accuracy of the drag data from the small-scale models as estimated from experience with previous models is of the order of ± 0.001 in C_D and ± 0.01 in M.

RESULTS AND DISCUSSION

Flight Reynolds numbers based on wing mean aerodynamic chord $\bar{c}$ for the 1/5-scale model and longitudinal distance $L/12$ for each of the six small-scale models are presented in figure 5.

Friction-drag coefficients were estimated from the measured Reynolds number variation and compressible skin-friction coefficients obtained from reference 2 for all models in order to determine the magnitude of pressure-drag coefficients at supersonic speeds.

Large-Scale Model

Coefficients of total, internal, and base drag are presented in figure 6 along with base pressure coefficients, forebody external-drag coefficients, and estimated external-friction-drag coefficients, all as functions of Mach number.

The total-drag-coefficient curve presented in figure 6(a) was established, in part, by using unpublished data from the Langley 8-foot transonic tunnel (see section entitled "Instrumentation and Data Reduction"). Only the subsonic levels were made to agree, however, and it should be noted that the agreement at low supersonic speeds ($M = 1.05$) was excellent. A constant value of 0.0005 was obtained for internal-drag coefficients over the entire Mach number range of the tests. Relatively low values of internal drag were expected because of the large increase in duct area behind the inlets and because of the smooth variations in duct area. Base drag coefficients ranged from -0.0007 at high subsonic speeds to a maximum of 0.0020 at $M \approx 1.3$. Base pressures, however, were measured only on the portion of the base which was formed by the central body in the duct, that is, the base of the choking cup and the exit of the internal rocket motor (fig. 2(b)). Since base pressures were not measured on the annular area of the base of the fuselage at the duct-exit station, the external-forebody-drag data of figure 6(c) include a small amount of drag due to the annular base area of the fuselage shell. The value of the forebody external-pressure-drag coefficient C_{D_p} was 0.0183 at $M = 1.05$.

Figure 7 shows the variation in $C_{N_{trim}}$ and $C_{Y_{trim}}$ with Mach number for the model which had a preset elevon deflection of approximately 1.3° trailing edge up and 0° rudder deflection. An abrupt change in $C_{N_{trim}}$ occurred between Mach numbers 0.9 to 1.0.

Duct characteristics are illustrated in figure 8 for the model which was equipped with scaled inlets and a choked exit. The mass-flow ratios m/m_o presented exceed 1.0 primarily because the interior inlet area was used in the calculations (see table I).

Small-Scale Models

Results of six free-flight tests involving small (length, approximately 10 inches) equivalent bodies of revolution of four proposed modifications to the F-102 configuration are presented in figure 9. The curves for models 1 to 4 show the measured total drag coefficients for the four different shapes where the equivalent bodies of revolution were obtained from the transonic (M = 1.0) distribution of airplane cross-sectional area (see ref. 4). In order to illustrate the total-drag penalty associated with flight through transonic speeds and to minimize the effects of Mach number error, drag-rise values listed in table III are for a Mach number of 1.05. These values include base drag. The basic and 2-foot-fuselage-extension configurations produced no significant change in drag. The 7-foot extension, however, showed a reduction in external-pressure-drag coefficient of 0.0046 from that of the small-scale rocket-propelled model configuration. In an attempt to evaluate the drag of two of the four different airplane shapes at M = 1.2, the contractor supplied two equivalent bodies of revolution which were shaped to correspond to a representative area distribution of the airplane derived for M = 1.2. The results of these tests (models 5 and 6) are also shown in figure 9. Presented also are the estimated friction-drag coefficients used to determine drag-rise increments.

Results of the helium-gun tests relative to the 1/5-scale rocket-propelled model configuration are presented in figure 10. The first part shows the forebody external-pressure-drag coefficients C_{D_p} obtained from the 1/5-scale rocket-propelled model which had a nearly constant value of approximately 0.0183 within the supersonic Mach number range of the tests. Drag-rise Mach number (where the slope of the drag curve $dC_D/dM = 0.1$) occurred at $M \approx 0.92$. The second part of figure 10 compares the external-pressure-drag coefficients $C_{D_{p+b}}$ of the 1/5-scale rocket-propelled model with those of the corresponding equivalent bodies of revolution for M = 1.0 (model 2) and 1.2 (model 5). The transonic (M = 1.0) equivalent body indicated a drag coefficient of about 96 percent of that shown for the 1/5-scale model at M = 1.05. The M = 1.2 equivalent body, however, had a drag coefficient of only 79 percent of the value indicated by the 1/5-scale model at M = 1.2.

It appears that, from the results of model 5, attempting to represent a complete airplane in the form of a single equivalent body of revolution

is not feasible for Mach numbers greater than 1.0, that is, where this single body shape is obtained from the average of the areas at each station of the many bodies determined by rotation of the inclined, parallel Mach planes around the longitudinal axis.

CONCLUSIONS

A 1/5-scale rocket-propelled model of the Convair F-102 configuration was tested in free flight in order to evaluate the interference-free, zero-lift drag through the transonic speed range at high Reynolds numbers. Several equivalent bodies of revolution models representing four proposed modifications to the airplane shape were flight tested to determine zero-lift drag rise.

1. For the 1/5-scale model the forebody external-pressure-drag coefficient at a Mach number of 1.05 was approximately 0.0183.

2. For the models designed to correspond to the area distribution at a Mach number of 1.0, the relatively small changes in fuselage shape incorporated in the basic and 2-foot-fuselage-extension configurations produced no significant changes in drag rise at transonic speeds ($M = 1.05$) from that of the 1/5-scale rocket-propelled model configuration. The 7-foot-fuselage-extension configuration, however, showed substantial reduction in drag rise at $M = 1.05$ (0.0046 decrease in drag rise).

Langley Aeronautical Laboratory,
National Advisory Committee for Aeronautics,
Langley Field, Va., March 29, 1954.

Harvey A. Wallskog

Harvey A. Wallskog
Aeronautical Research Scientist

Approved: Joseph A. Shortal

Joseph A. Shortal
Chief of Pilotless Aircraft Research Division

DY

REFERENCES

1. Hall, James Rudyard: Comparison of Free-Flight Measurements of the Zero-Lift Drag Rise of Six Airplane Configurations and Their Equivalent Bodies of Revolution at Transonic Speeds. NACA RM L53J21a, 1954.

2. Van Driest, E. R.: Turbulent Boundary Layer in Compressible Fluids. Jour. Aero. Sci., vol. 18, no. 3, Mar. 1951, pp. 145-160, 216.

3. Stoney, William E., Jr.: Some Experimental Effects of Afterbody Shape on the Zero-Lift Drag of Bodies for Mach Numbers Between 0.8 to 1.3. NACA RM L53I01, 1953.

4. Whitcomb, Richard T.: A Study of the Zero-Lift Drag-Rise Characteristics of Wing-Body Combinations Near the Speed of Sound. NACA RM L52H08, 1952.

TABLE I

DIMENSIONAL DATA FOR THE 1/5-SCALE ROCKET-PROPELLED MODEL OF THE CONVAIR F-102 CONFIGURATION

Wing:	
Area, total, sq ft	26.46
Span, in.	91.5
Mean aerodynamic chord, in.	55.5
Aspect ratio, total	2.2
Taper ratio	0
Root chord, in.	83.3
Tip chord, in.	0
Airfoil section	NACA 0004-65 (modified)
Angle of incidence, deg	0
Dihedral angle, deg	0
Sweepback leading edge, deg	60
Sweepforward trailing edge, deg	5
Elevon area, total, sq ft	2.63
Elevon deflection, average, trailing edge up, deg	1.3
Vertical Tail:	
Area, exposed, sq ft	2.73
Span, panel, in.	20.8
Aspect ratio (panel)	1.1
Taper ratio	0
Root chord, in.	37.8
Tip chord, in.	0
Airfoil section	NACA 0004-65 (modified)
Sweepback leading edge, deg	60
Sweepforward trailing edge, deg	5
Fuselage:	
Length, overall, in.	123.4
Maximum width, in.	15.6
Maximum height	
With canopy, in.	16.5
Without canopy, in.	15.6
Base area	
Total, sq in.	90.1
Central body in duct exit, sq in.	53.2
Duct:	
Inlet area (interior) ($\alpha \approx 5^{\circ}$, $\beta = 0^{\circ}$), sq in.	26.8
Inlet area (inlet lip contour projected on a plane normal to the reference line), sq in.	29.3
Exit area ($\alpha = 2^{\circ}$, $\beta = 0^{\circ}$), sq in.	26.8

[redacted]

TABLE II

WEIGHT, BALANCE, AND INERTIA DATA FOR THE 1/5-SCALE ROCKET-PROPELLED MODEL OF THE CONVAIR F-102 AIRPLANE

Weight (propellant expended), lb	352
Wing loading, lb/sq ft	13.3
Center of gravity	
Longitudinal, percent $\bar{c}$	21.9
Lateral, from plane of symmetry, in.	-0.1
Vertical, from reference line, in.	-1.4
Moment of inertia:	
About X principal axis, slug-ft^2	8
About Y principal axis, slug-ft^2	75
About Z principal axis, slug-ft^2	51
Principal axis inclination (down at nose from wing chord plane), deg	$\approx$ 1.2

TABLE III

EXTERNAL-PRESSURE-DRAG COEFFICIENTS[1] AT M = 1.05 FROM FREE-FLIGHT TESTS OF FOUR CONVAIR F-102 CONFIGURATIONS

Configuration	Small-scale model	External-pressure-drag coefficient	
		Small-scale equivalent body of revolution	1/5-scale rocket-propelled model
Basic fuselage	1	0.0179	------
Rocket model	2	.0183	0.0190
2-foot fuselage extension	3	.0181	------
7-foot fuselage extension	4	.0137	------

[1]This parameter is a measure of drag rise and includes base drag.

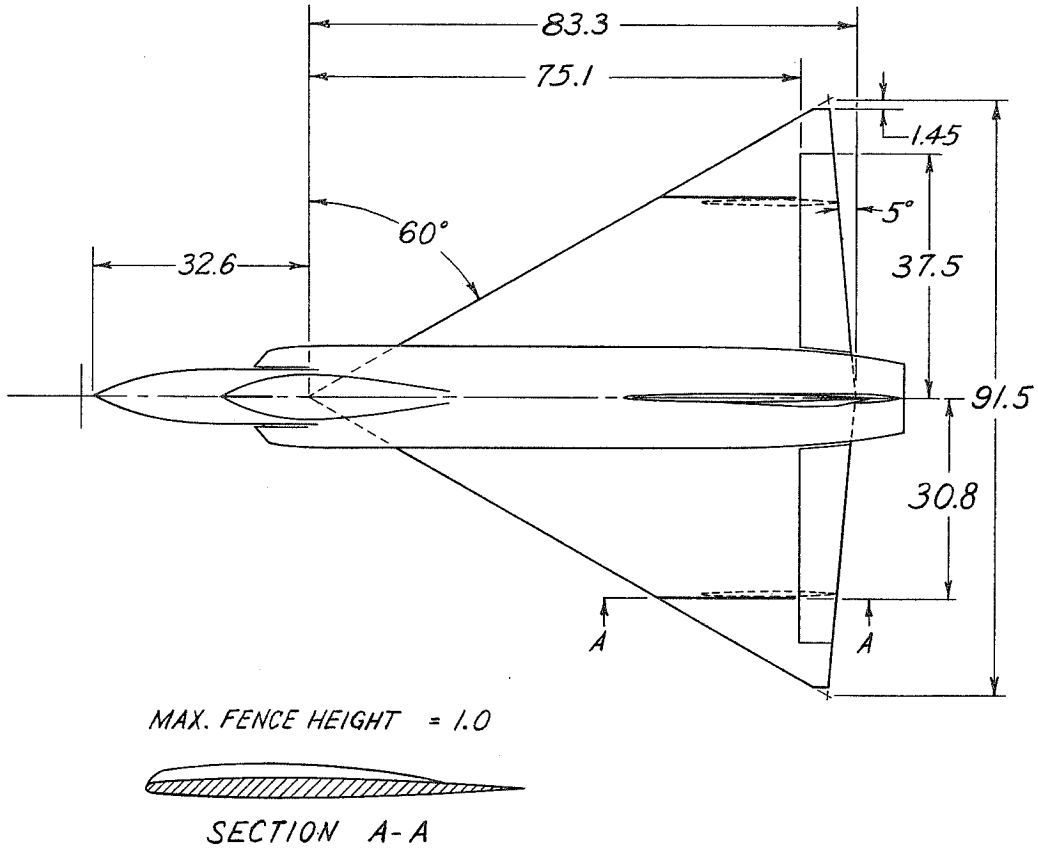

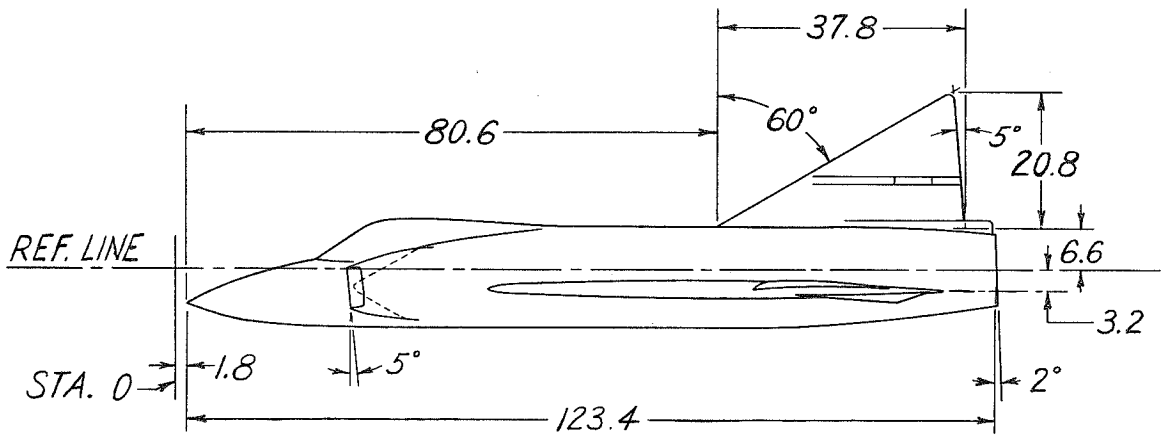

(a) Dimensional details of the 1/5-scale model. All dimensions are in inches.

Figure 1.- General arrangement of the 1/5-scale rocket-propelled model of the Convair F-102 configuration.

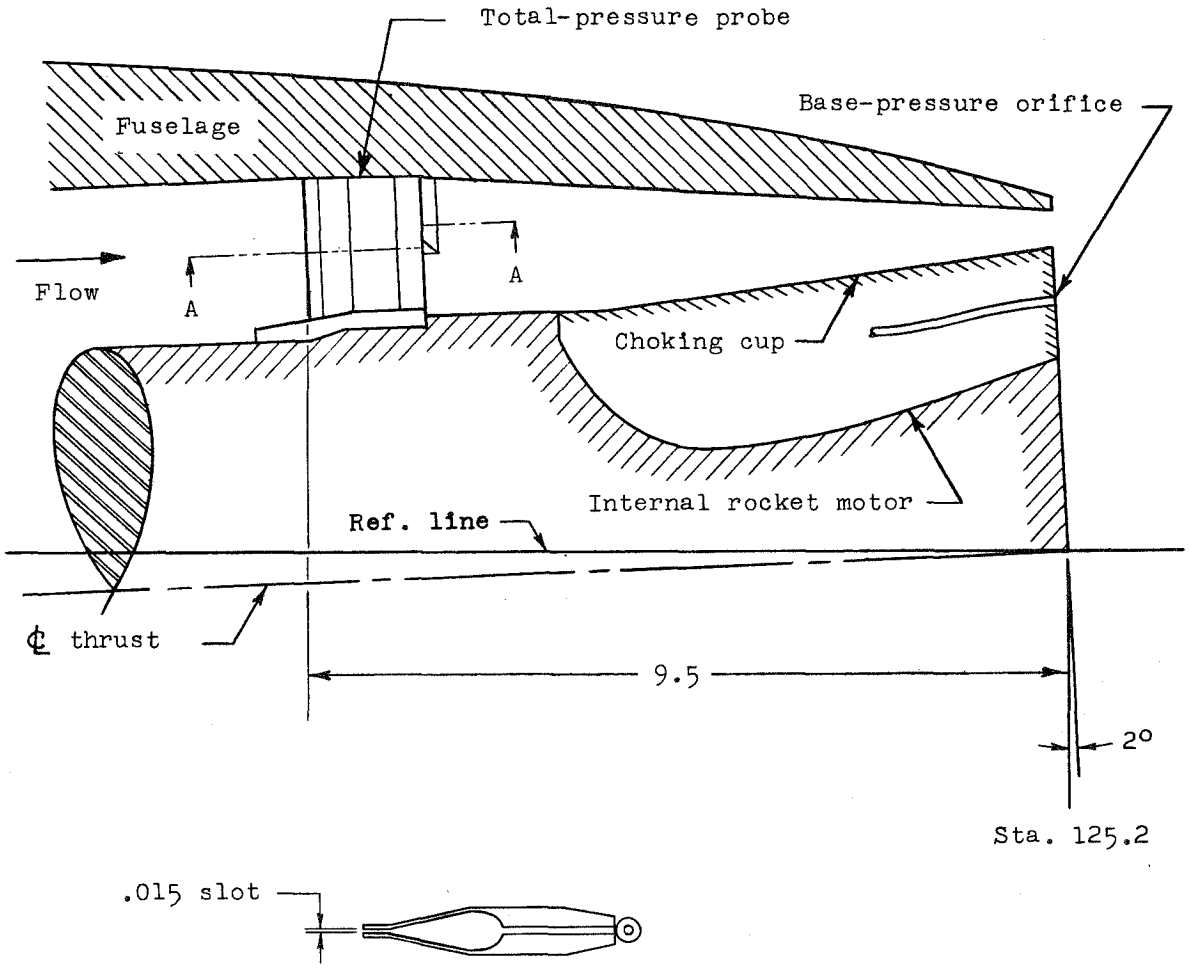

Section A-A

(b) Installation of duct-exit total-pressure probe.

Figure 1.- Continued.

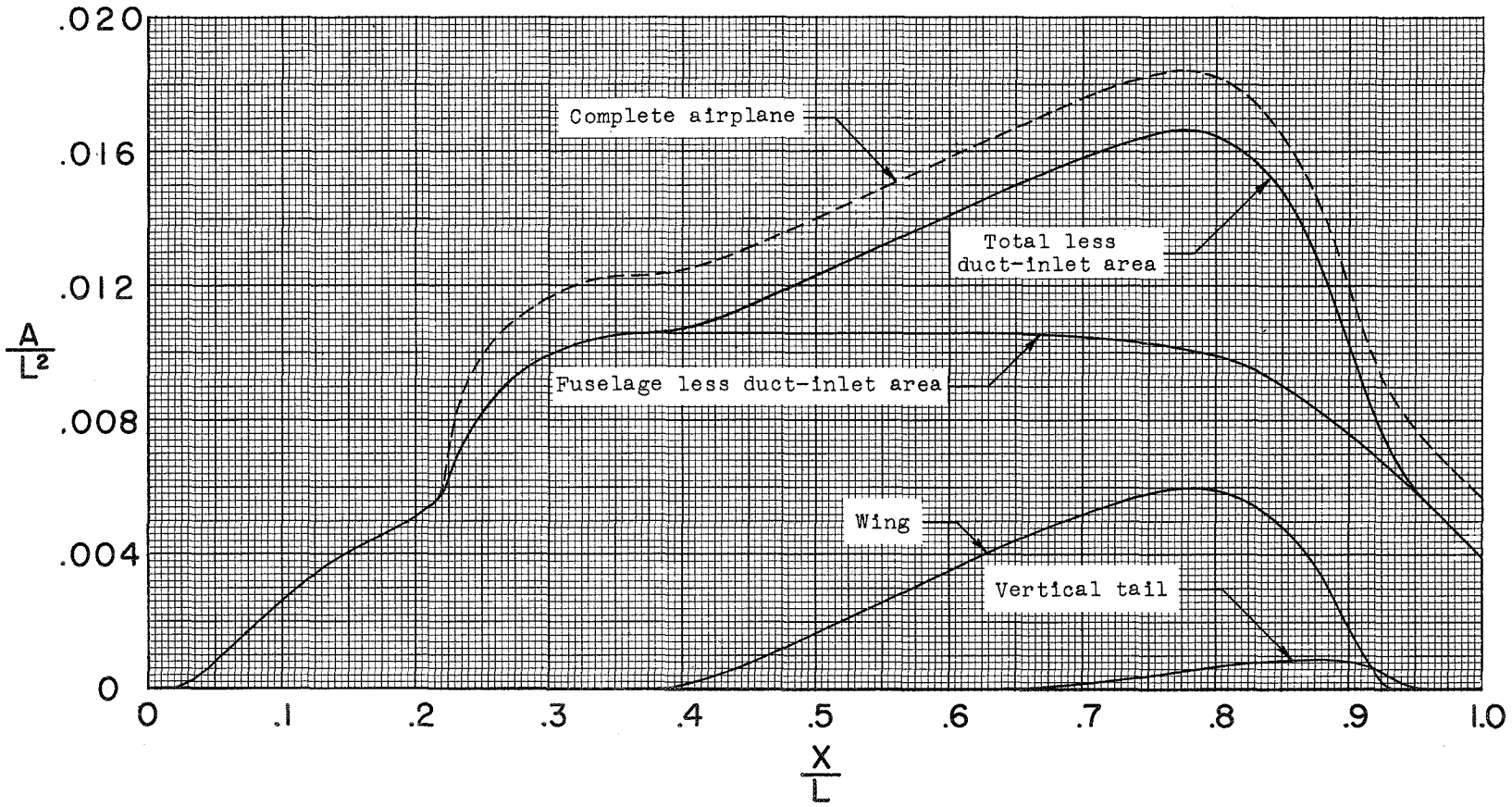

(c) Longitudinal distribution of cross-sectional area. L = 125.2 inches.

Figure 1.- Concluded.

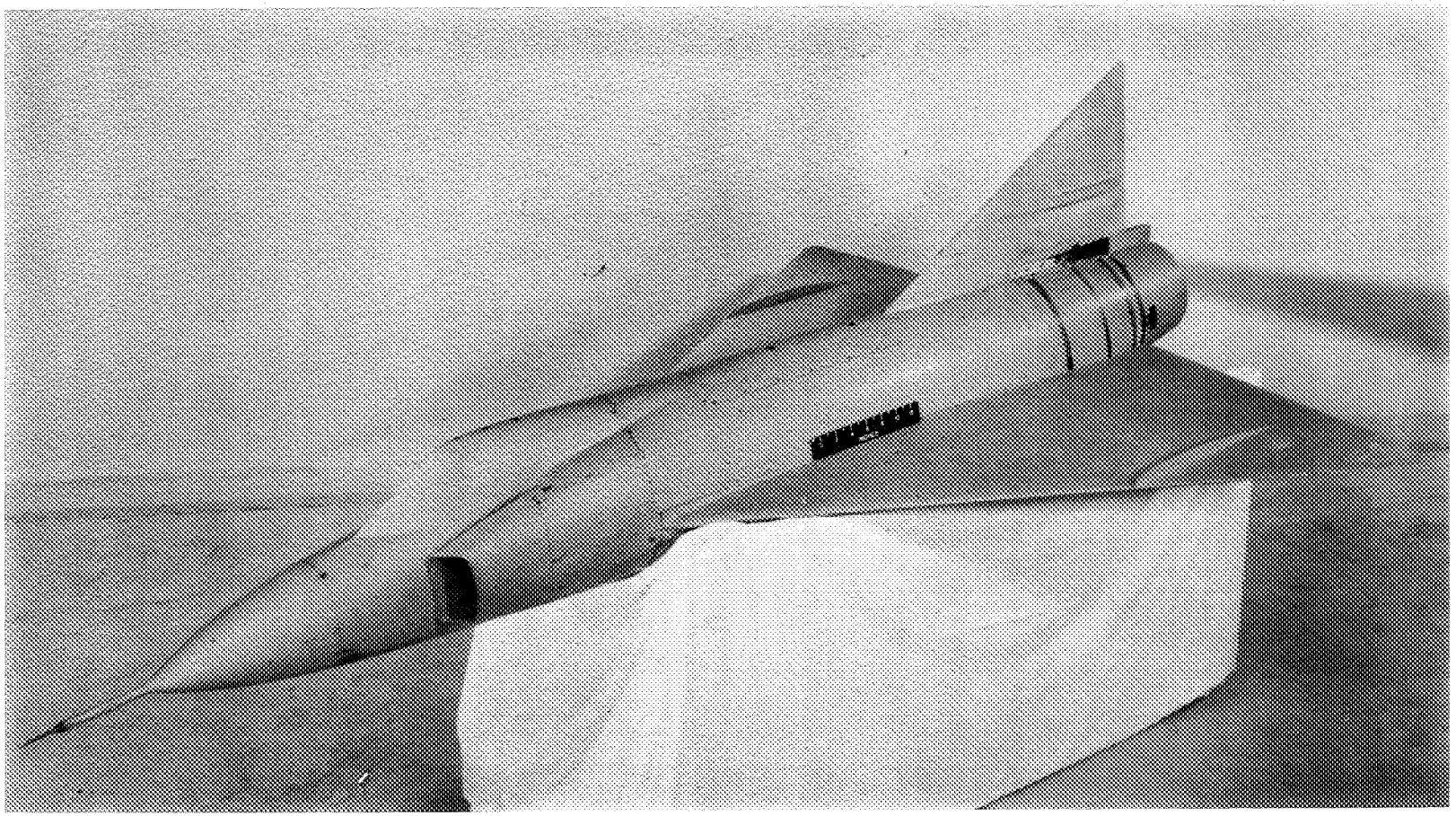

L-81068

(a) Overall view of model.

Figure 2.- Photographs of the 1/5-scale model of Convair F-102 airplane.

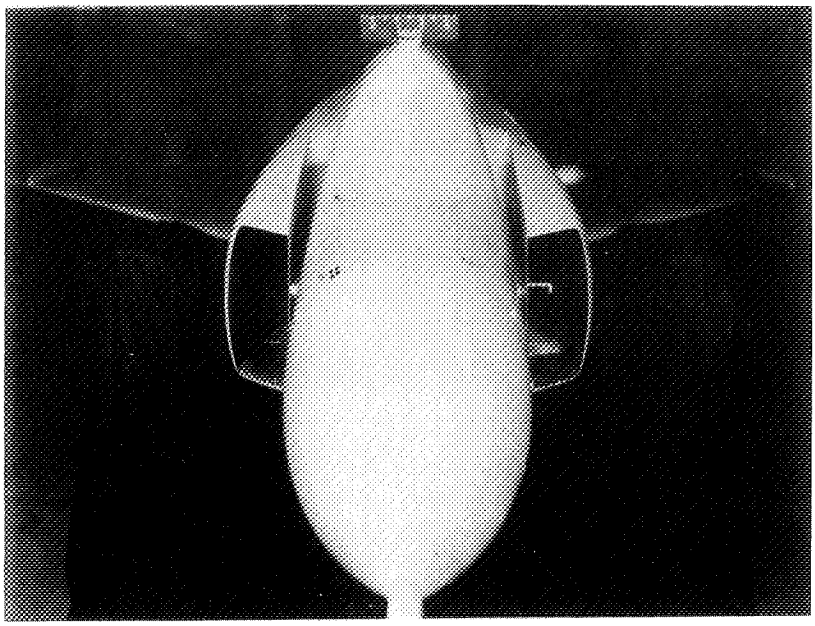

L-81064.1

(b) Forward view showing duct inlets and boundary layer splitters and canopy.

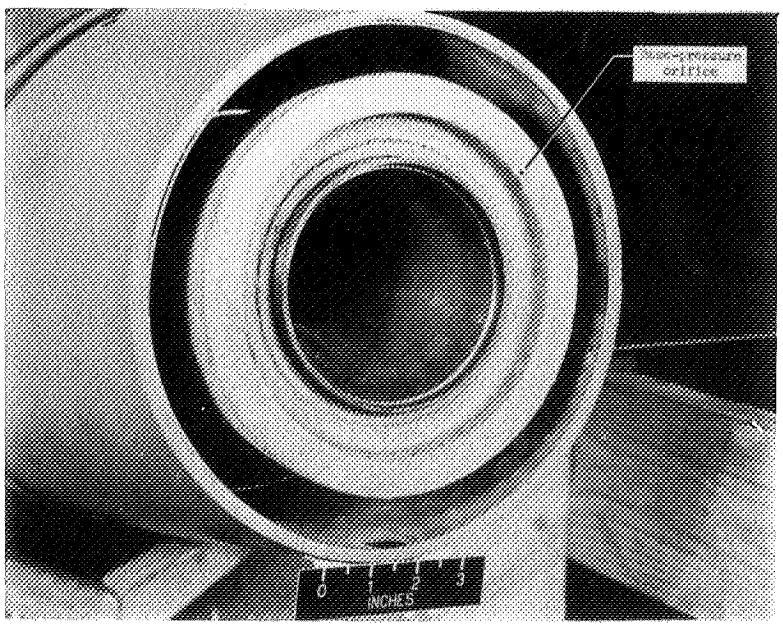

L-81067.1

(c) View showing duct exit with choking cup in place.

Figure 2.- Continued.

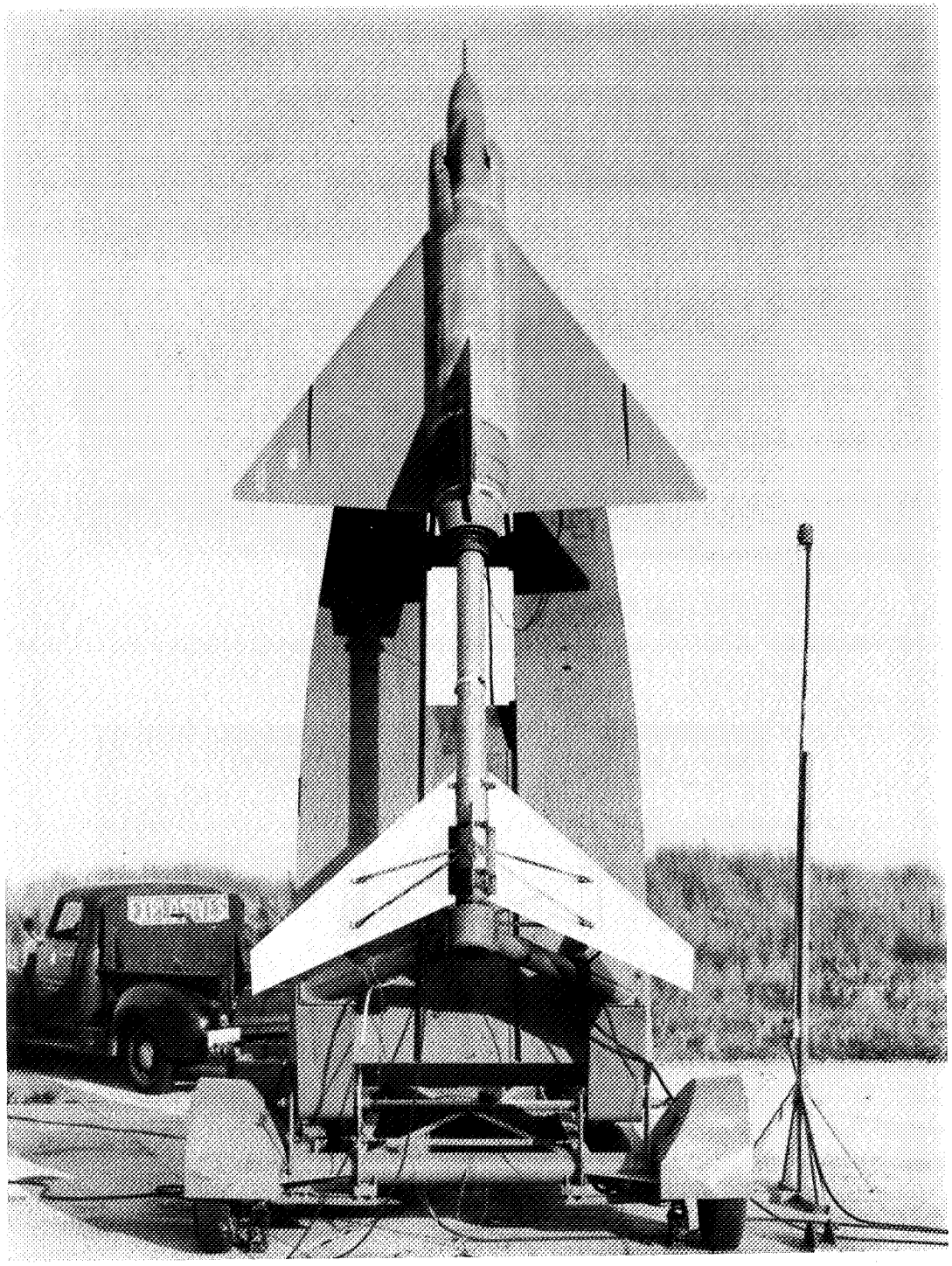

L-81319

(d) General view of the model and booster rocket on the launcher.

Figure 2.- Concluded.

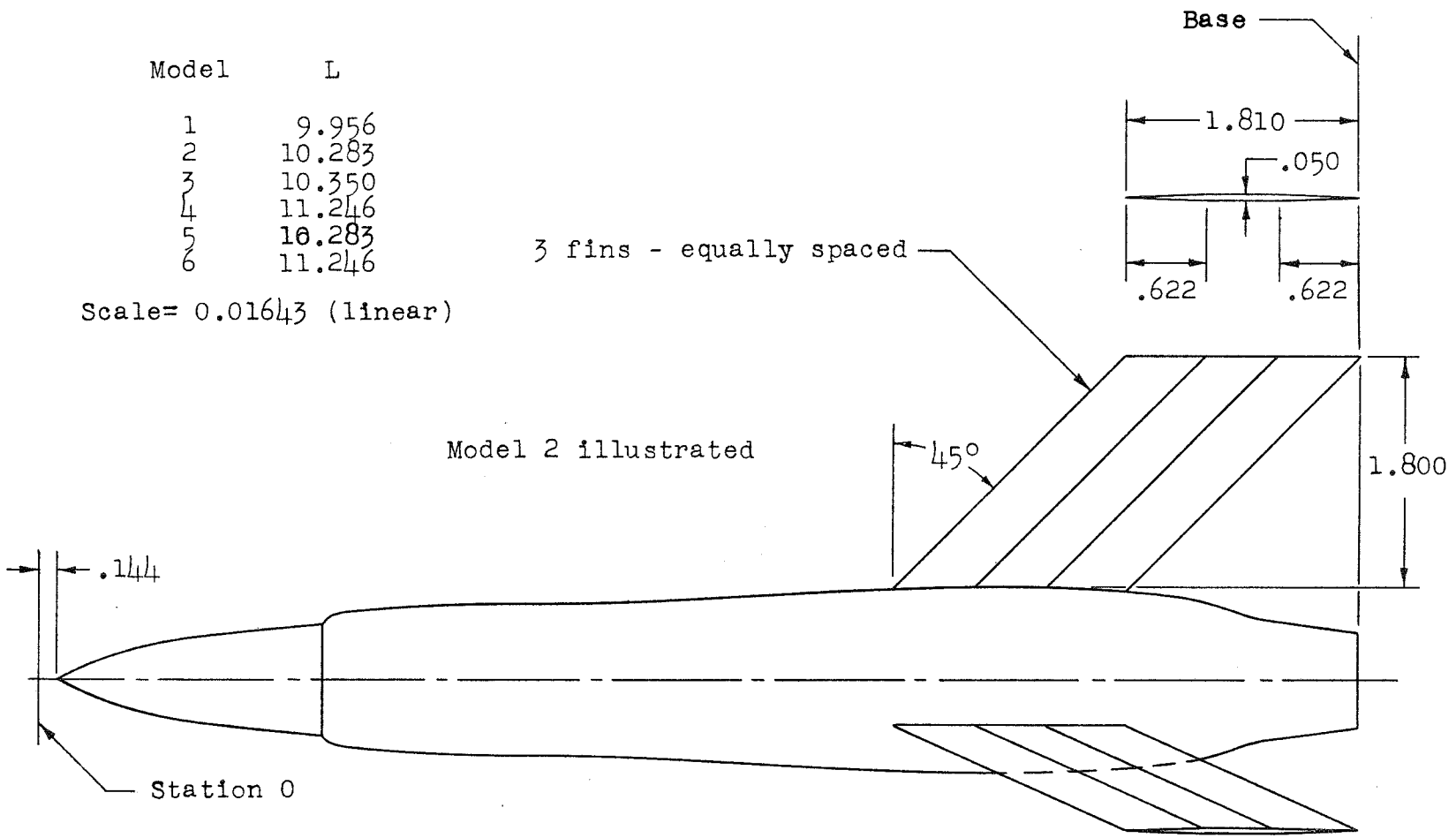

(a) Size, shape, and location of the model stabilizing fins. Same for models 1 to 6. Dimensions are in inches.

Figure 3.- General arrangement and shapes of the small-scale equivalent bodies of revolution.

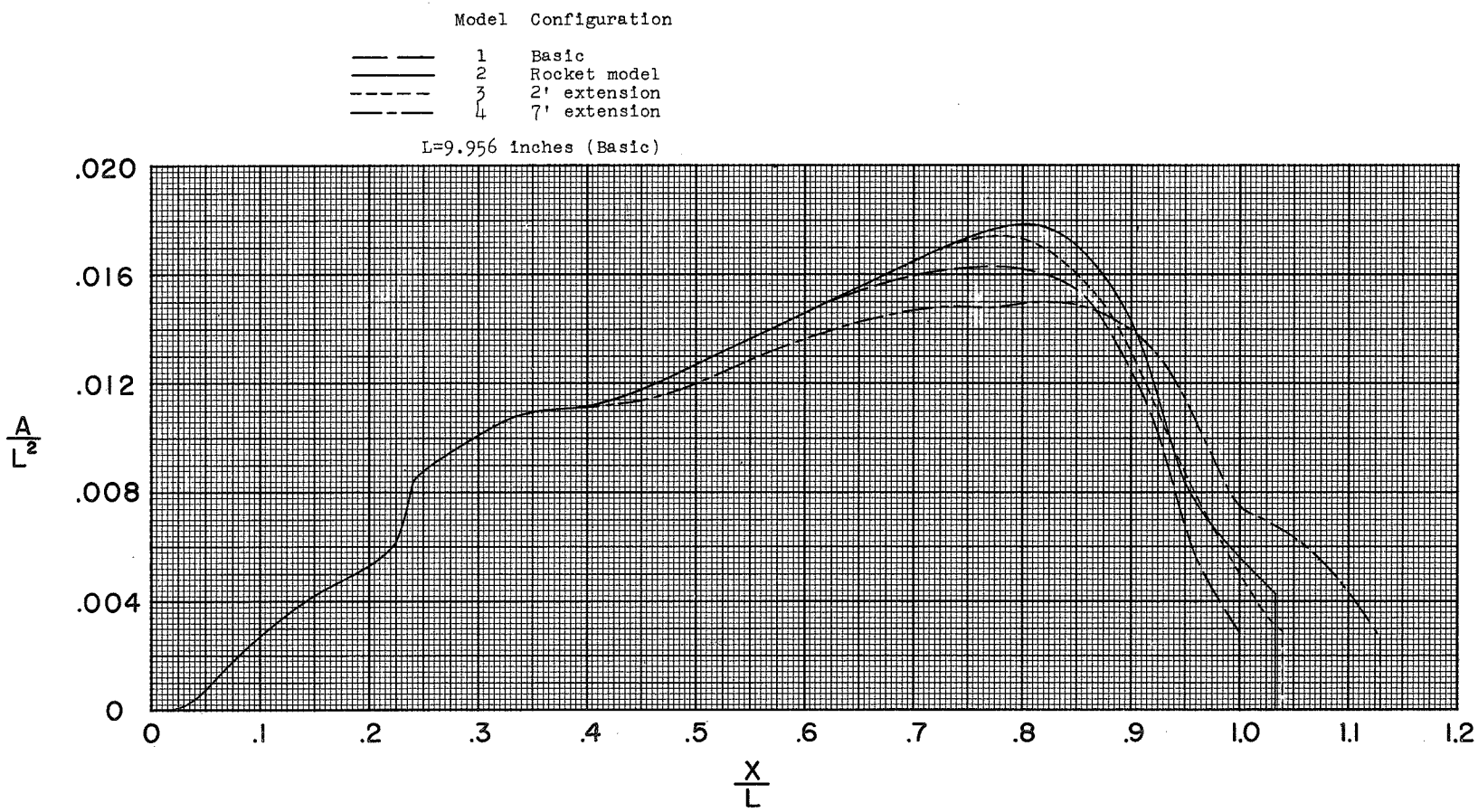

(b) Longitudinal distribution of cross-sectional area for models 1 to 4 (corresponds to each airplane configuration at Mach number M of 1.0 and a mass-flow ratio m/m_o of 1.0).

Figure 3.- Continued.

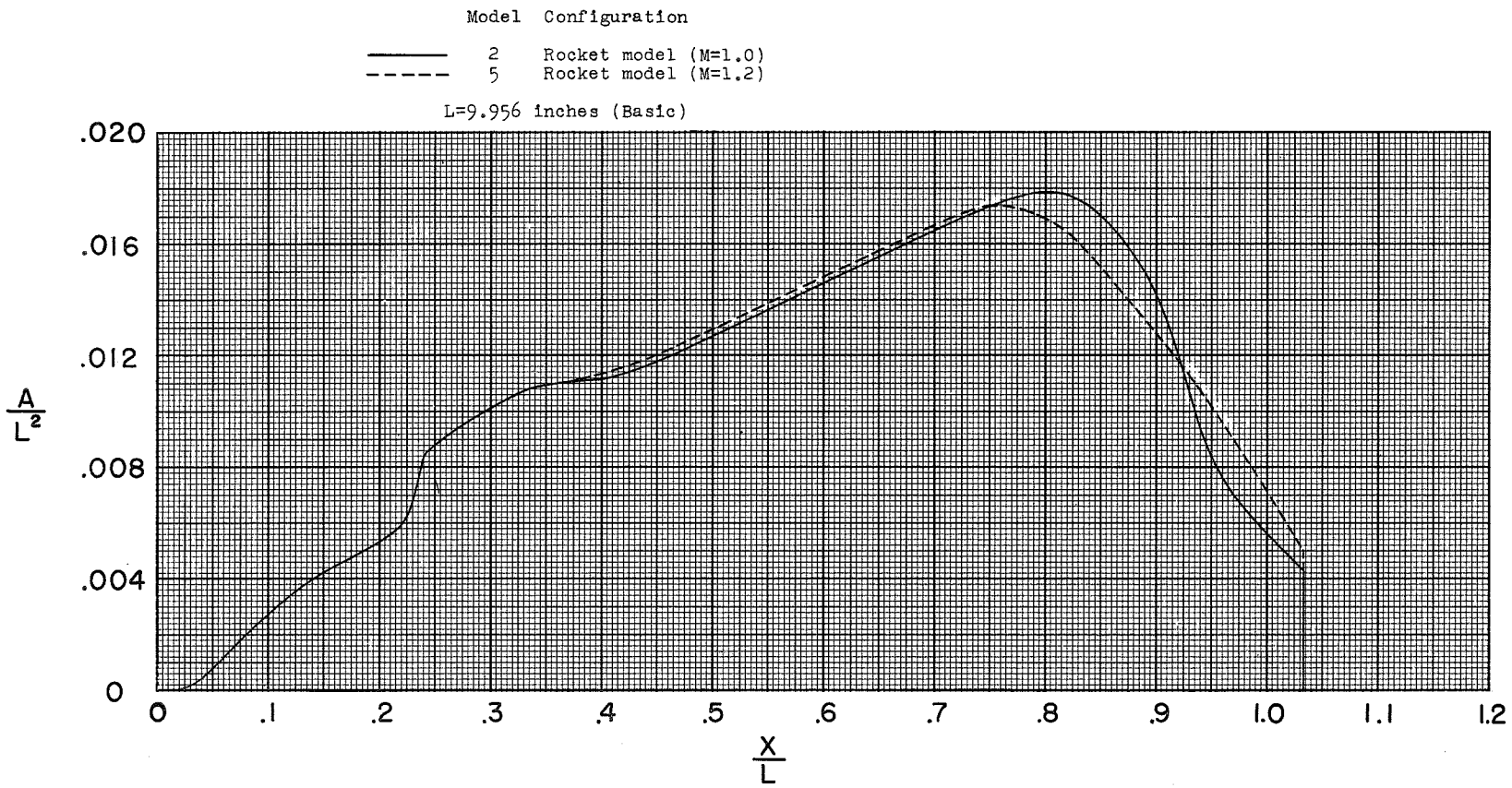

(c) Comparison of the area distribution at Mach numbers M of 1.0 (model 2) and 1.2 (model 5) for the rocket-propelled model configuration.

Figure 3.- Continued.

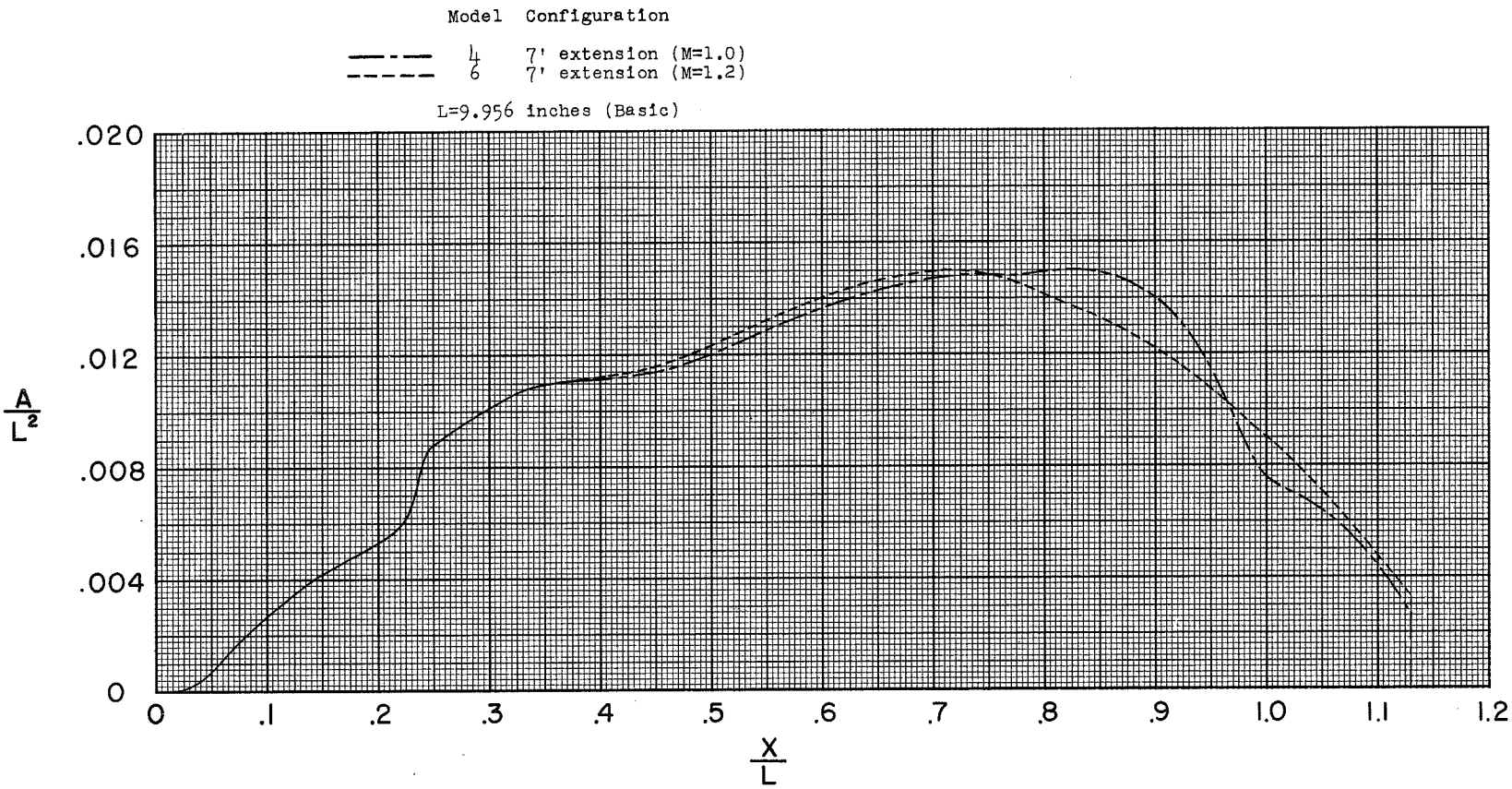

(d) Comparison of the area distribution at Mach numbers M of 1.0 (model 4) and 1.2 (model 6) for the 7-foot extension configuration.

Figure 3.- Concluded.

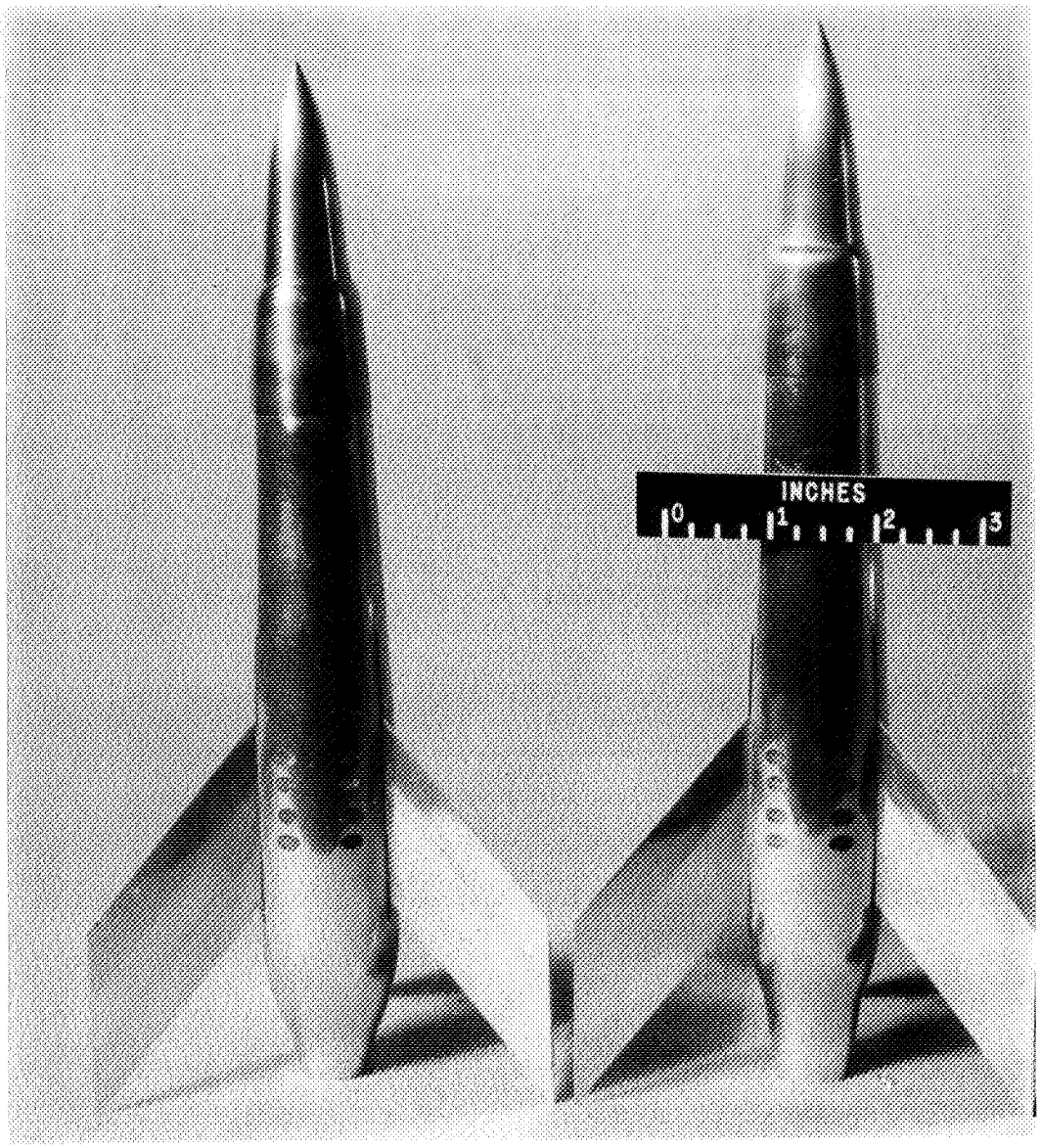

L-80864

(a) Models 1 and 2.

Figure 4.- Photographs of typical small-scale equivalent bodies of revolution.

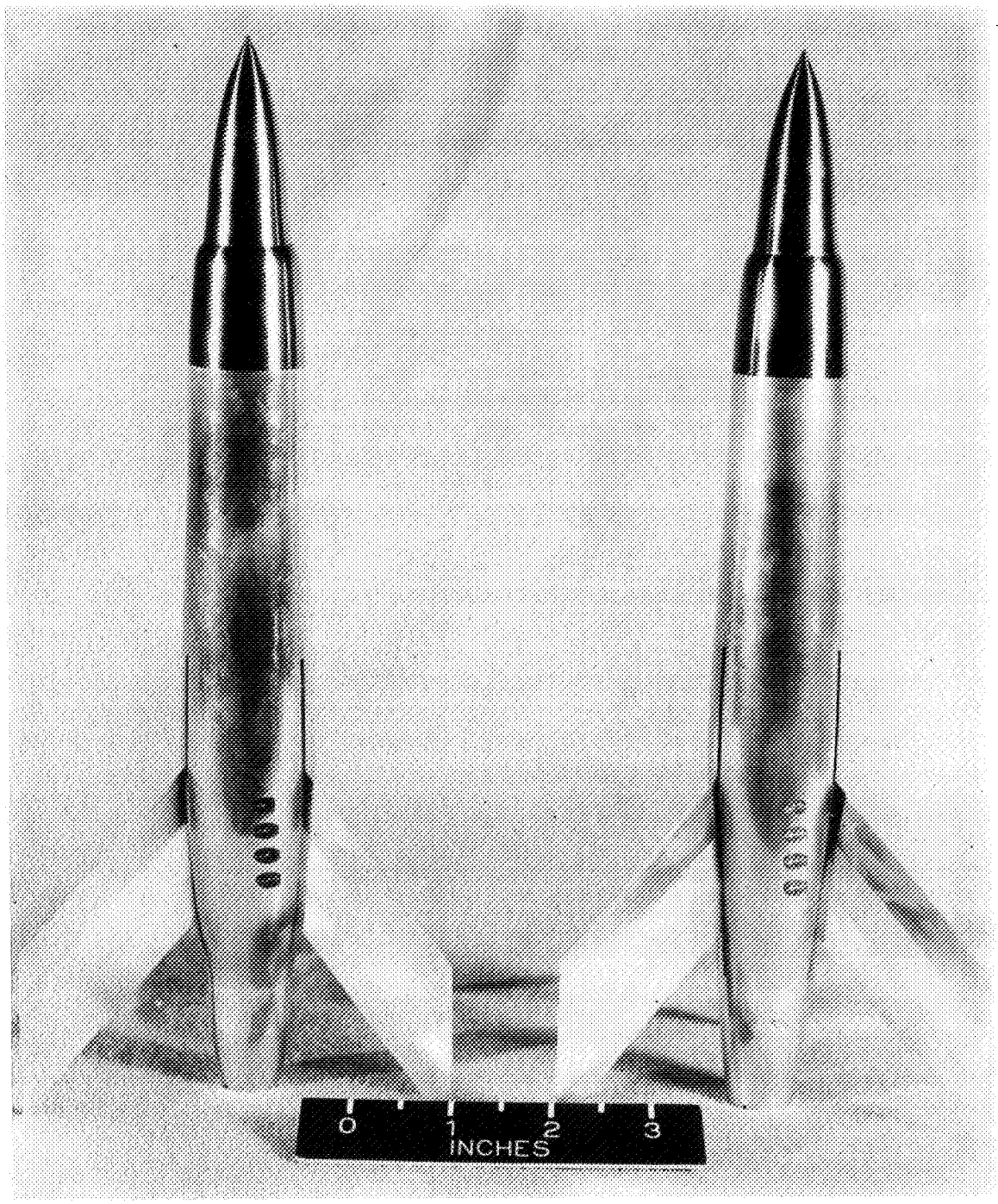

L-81776

(b) Models 4 and 6.

Figure 4.- Concluded.

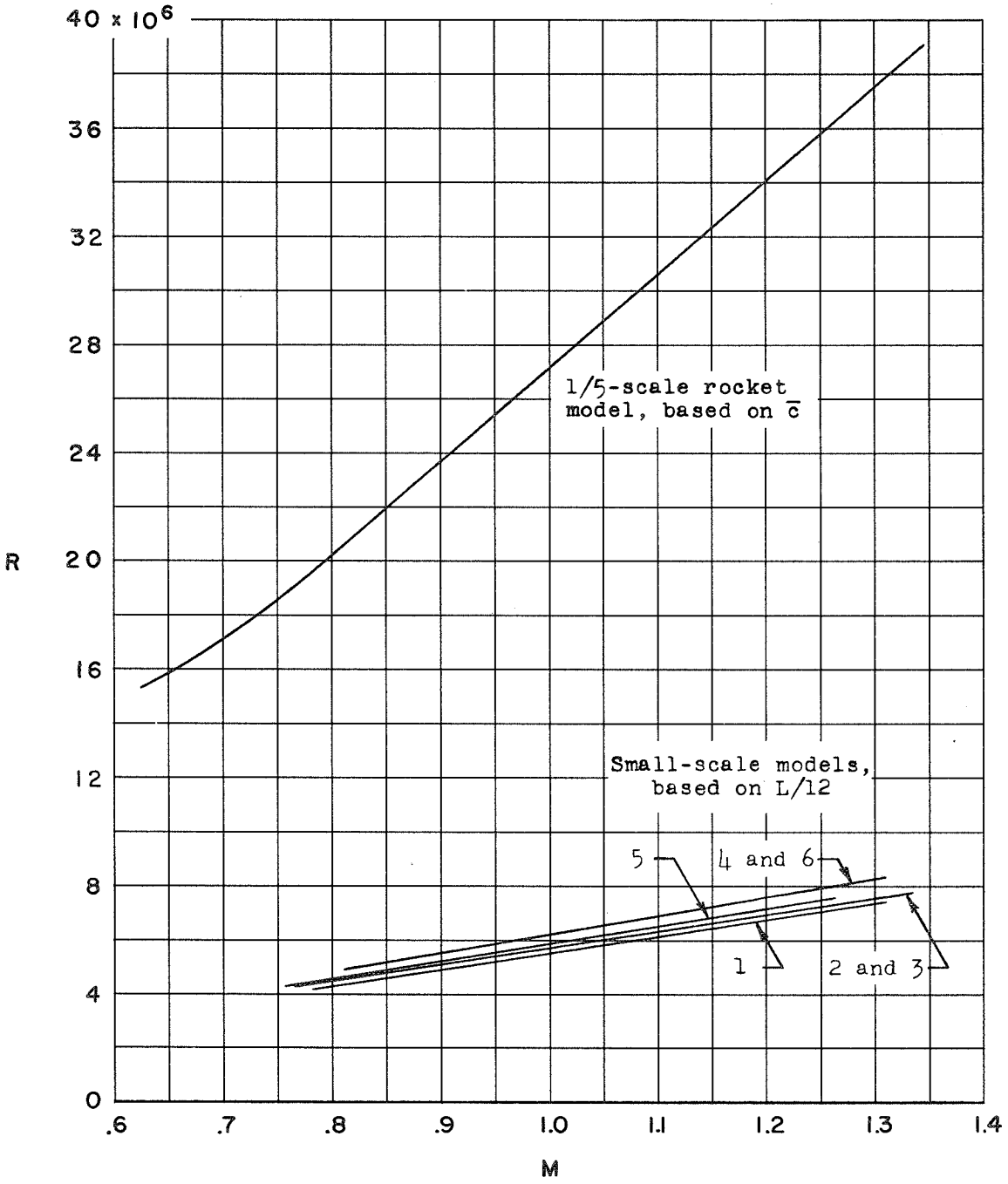

Figure 5.- Reynolds number R plotted as a function of Mach number M for the 1/5-scale rocket-propelled model and the small-scale models.

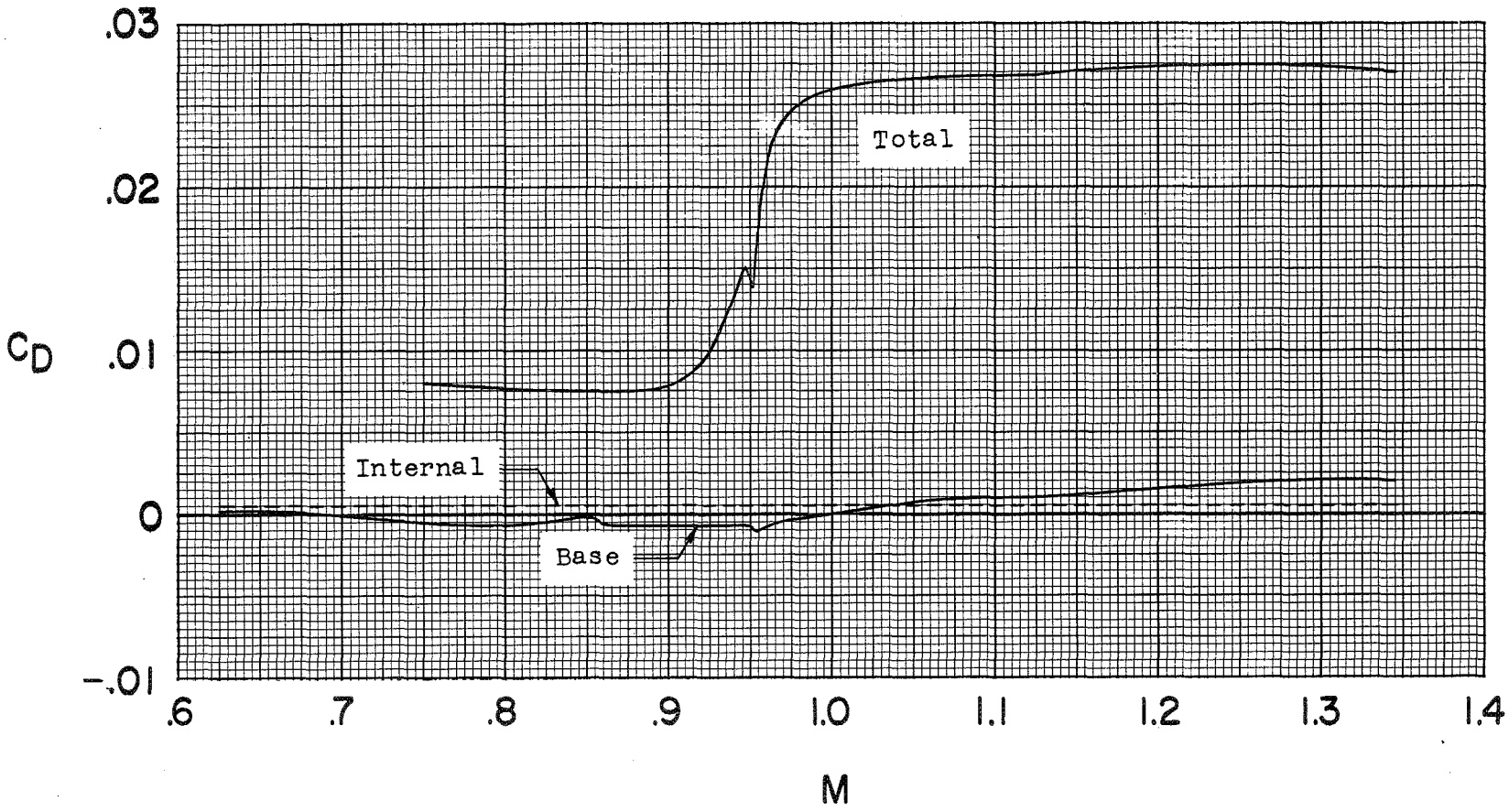

(a) Total C_D, internal C_{D_I}, and base C_{D_b} drag coefficients.

Figure 6.- Variation with Mach number of the total, internal, and base drag coefficients, base pressure coefficients, and external-drag coefficients of the 1/5-scale rocket-propelled model as measured during free flight.

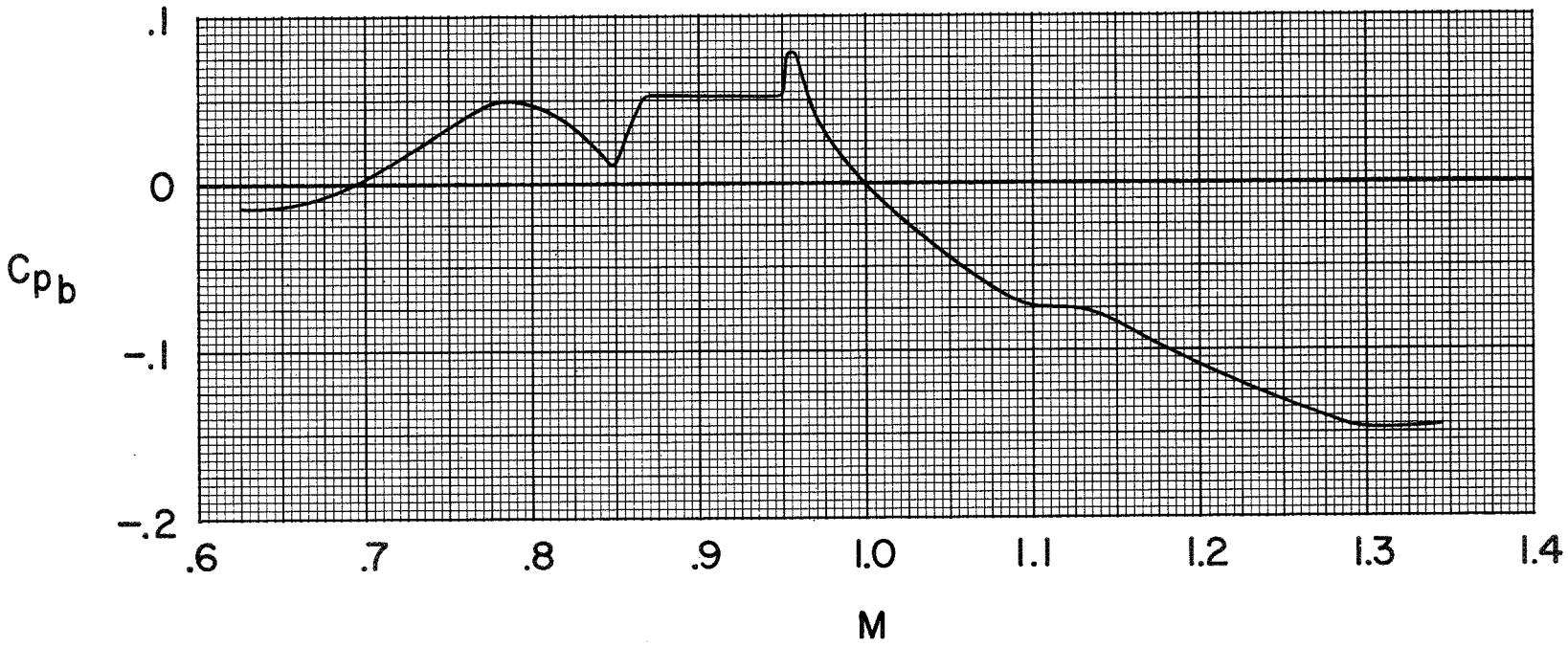

(b) Base pressure coefficients.

Figure 6.- Continued.

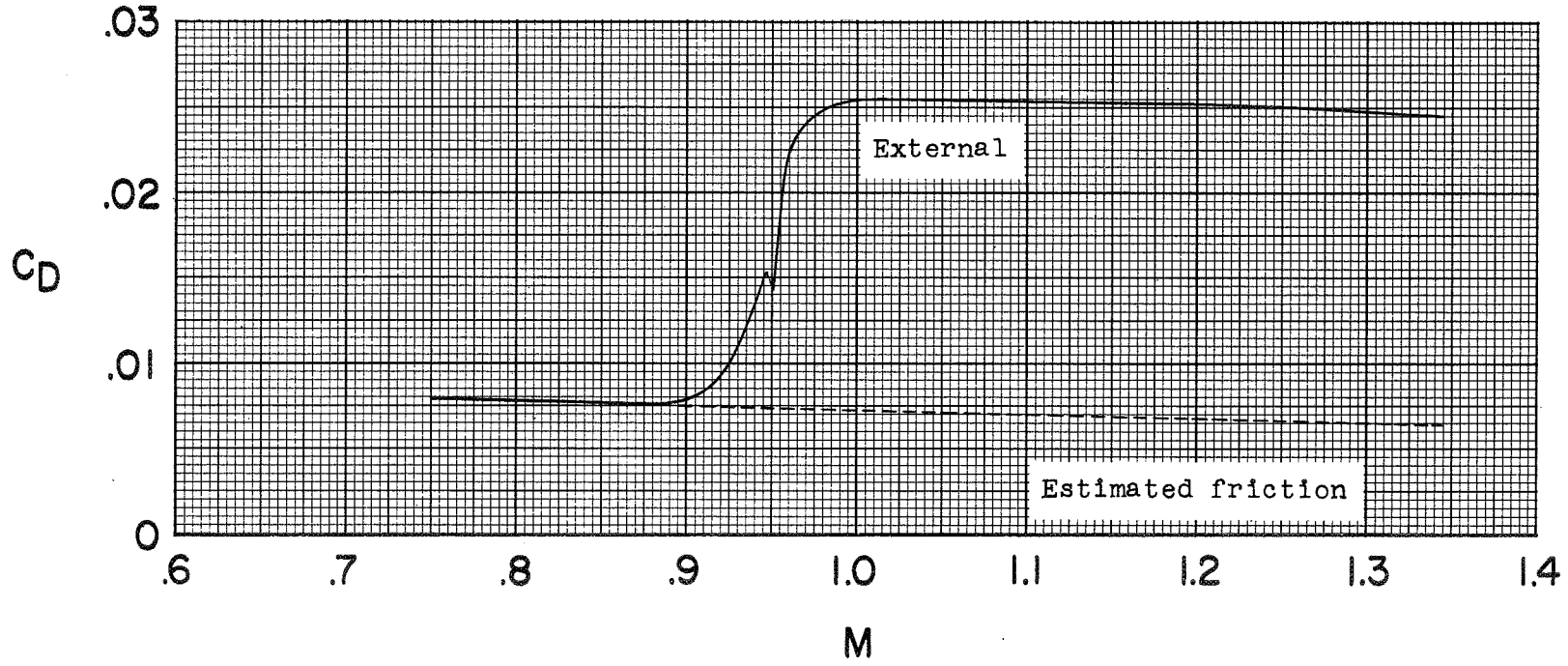

(c) External-forebody drag coefficients C_{D_E} and estimated external friction-drag coefficients C_{D_f}.

Figure 6.- Concluded.

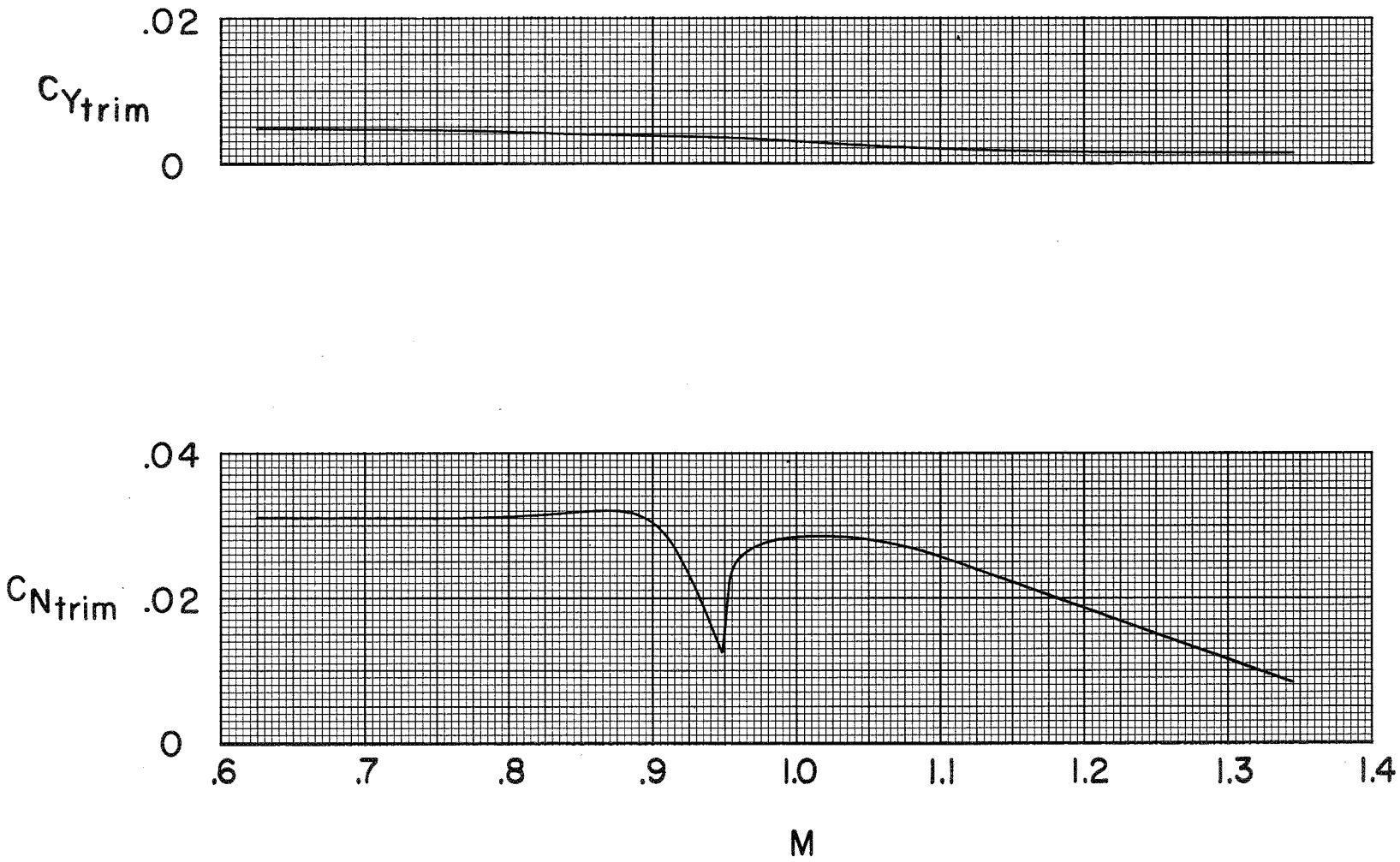

Figure 7.- Changes in lateral C_Y and longitudinal C_N trim with Mach number M for the 1/5-scale rocket-propelled model. Elevon deflection, 1.3°; trailing edge up; rudder deflection, 0°.

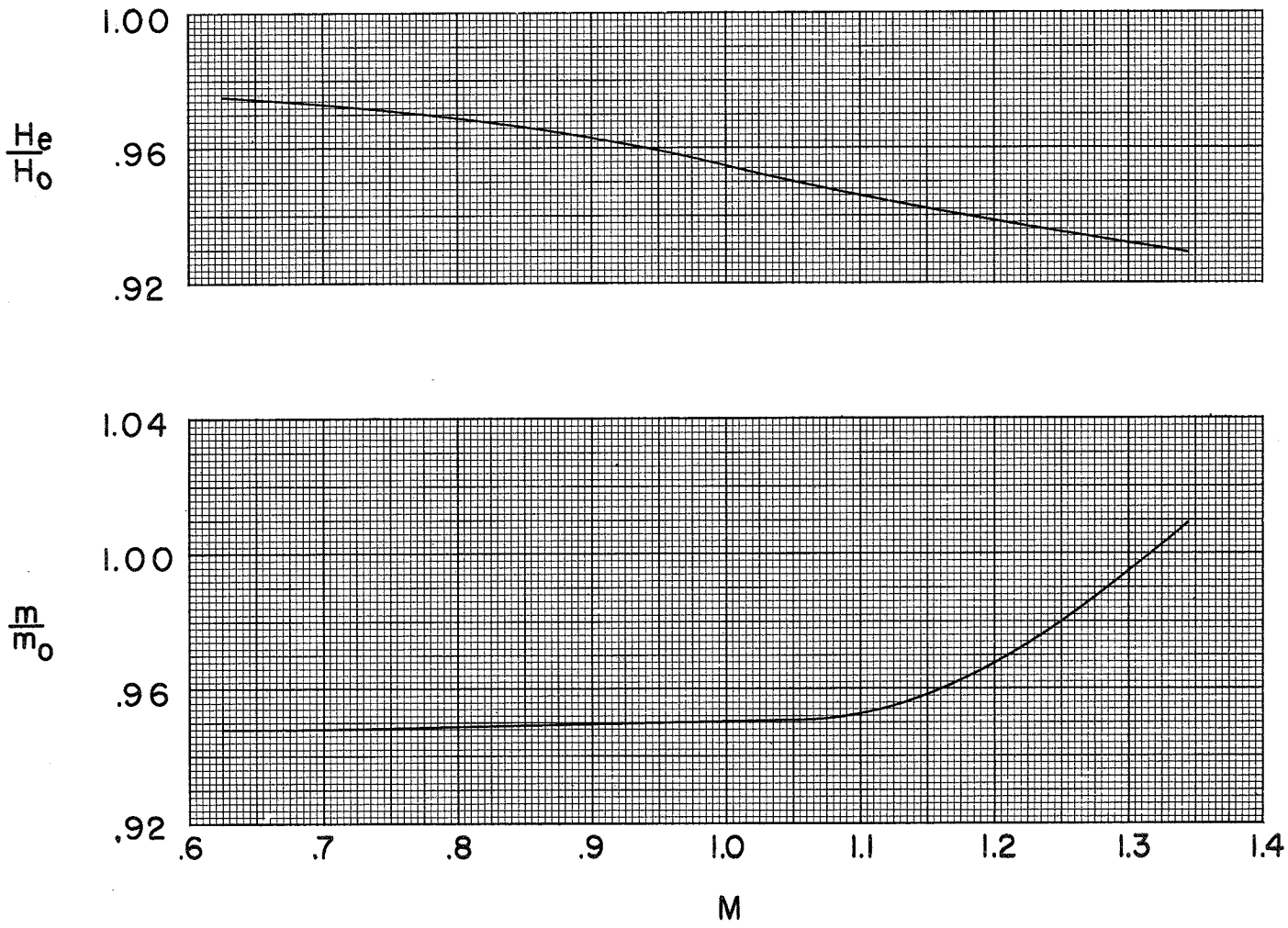

Figure 8.- Variation with Mach number M of the pressure recovery near the duct exit H_e/H_o and mass-flow ratio m/m_o for the 1/5-scale model (exit choked).

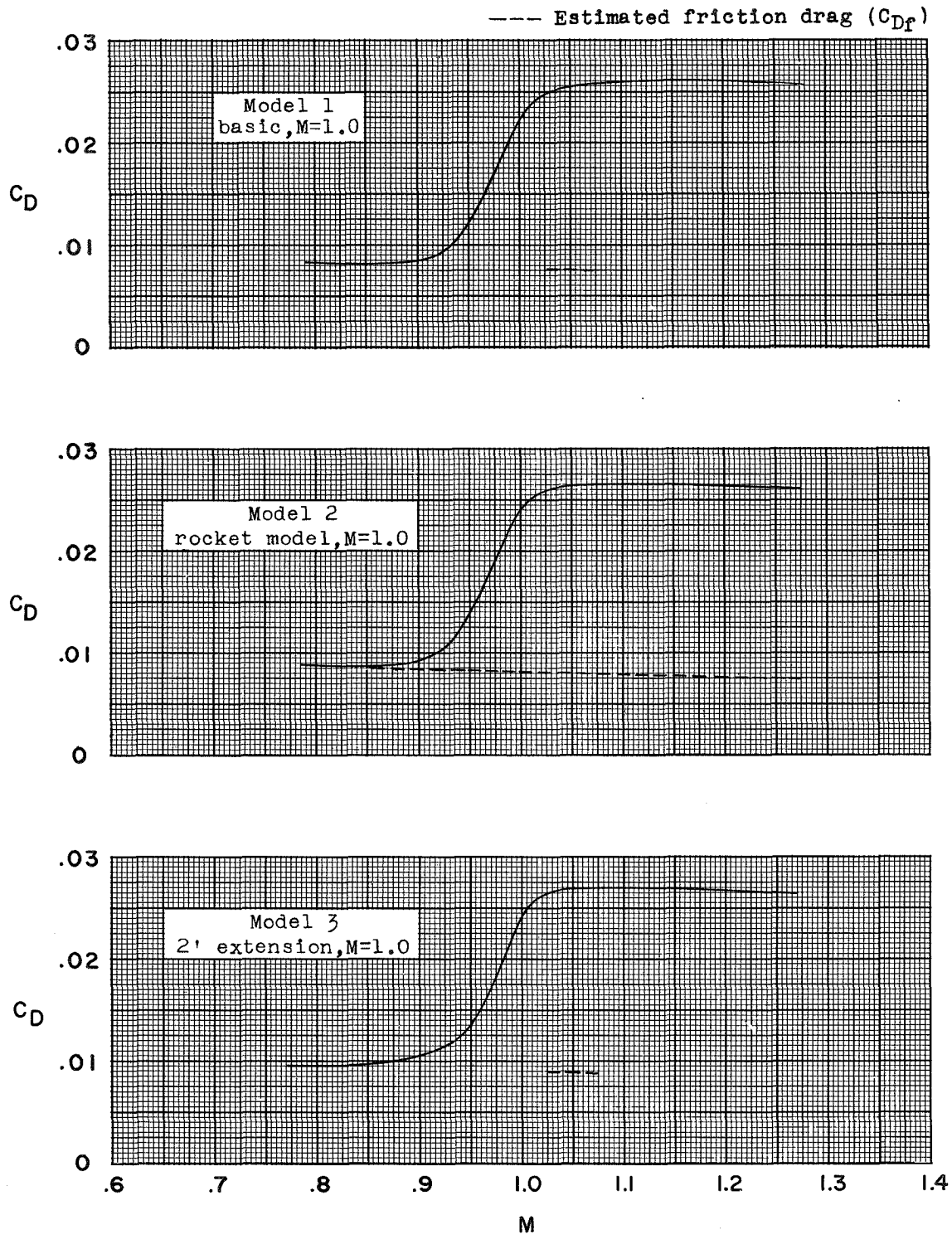

Figure 9.- Drag coefficients C_D based on scale wing area of equivalent bodies of revolution representing four different airplane configurations plotted against Mach number M.

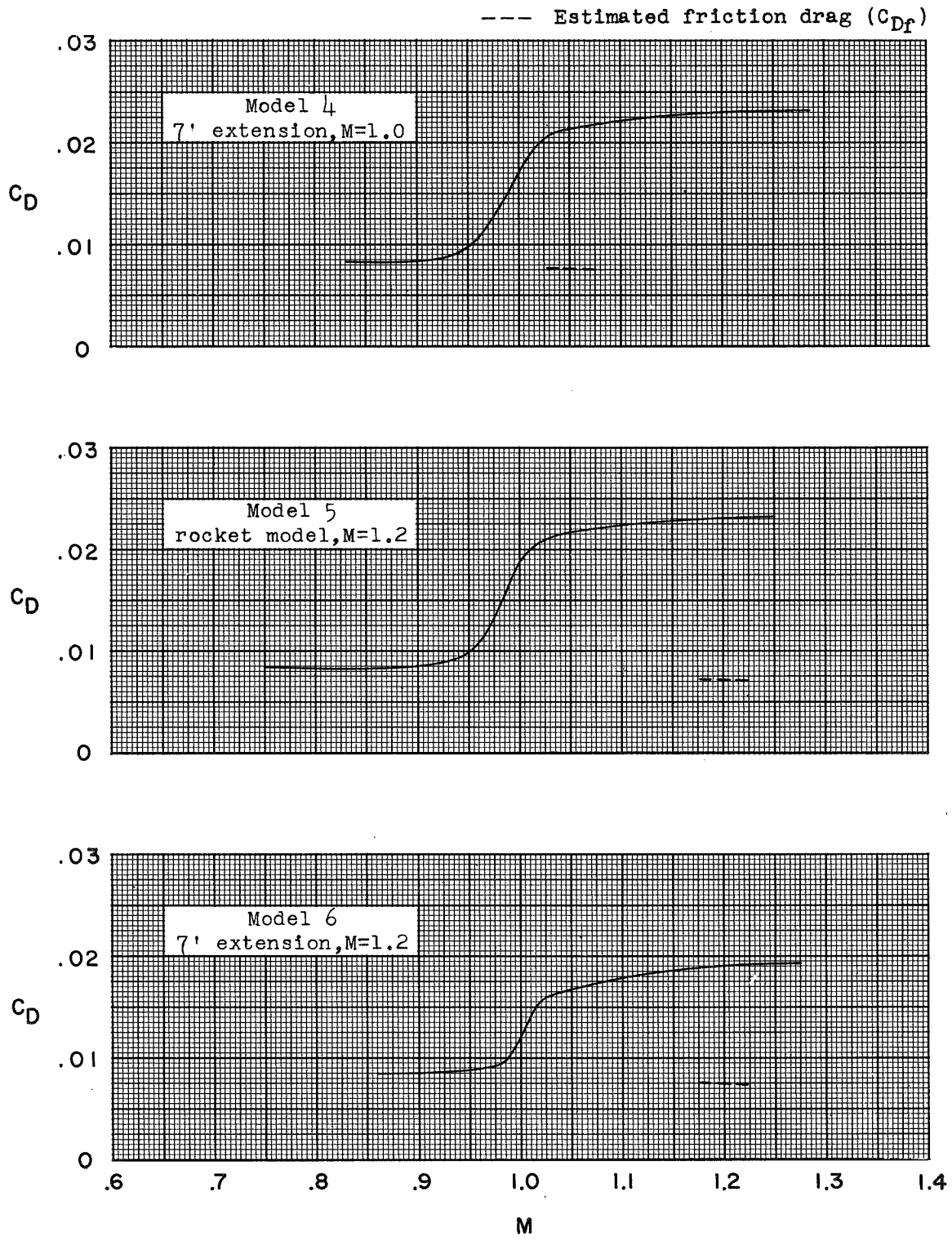

Figure 9.- Concluded.

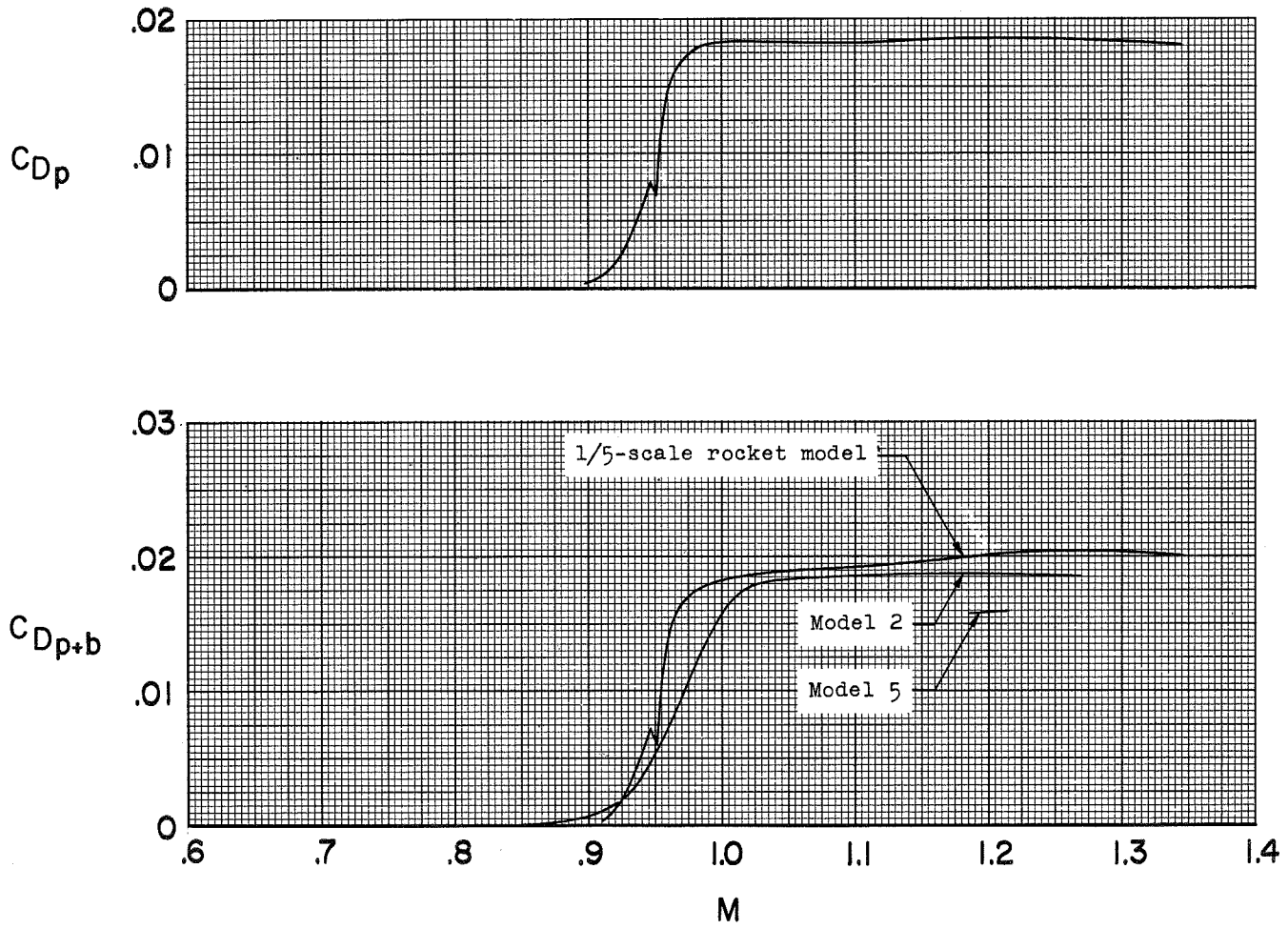

Figure 10.- Pressure drag coefficients C_{D_p} obtained from the 1/5-scale model and external pressure drag coefficients $C_{D_{p+b}}$ of the 1/5-scale rocket-propelled model compared with those obtained from the corresponding equivalent bodies of revolution.